

GAMMA DELTA T CELLS REGULATE INFLAMMATORY CELL INFILTRATION OF THE LUNG AFTER TRAUMA-HEMORRHAGE

Meenakshi Rani,* Qiong Zhang,* Richard F. Oppeltz,* and Martin G. Schwacha*†

*Department of Surgery, The University of Texas Health Science Center, San Antonio; and †US Army Institute of Surgical Research, Fort Sam Houston, Texas

Received 4 Nov 2014; first review completed 24 Nov 2014; accepted in final form 10 Feb 2015

ABSTRACT—Trauma-hemorrhage (TH) promotes acute lung injury (ALI) and other pulmonary-related complications in part through an exaggerated inflammatory response. Studies have implicated $\gamma\delta$ T cells in the development of inflammatory complications after major injury; however, it is unknown whether $\gamma\delta$ T cells play a role in the development of ALI after TH. To study this, C57BL/6 wild-type (WT) and δ TCR^{-/-} mice were subjected to TH or sham treatment. Lung injury was clearly evident at 2 h after TH, as evidenced by increased lung permeability, myeloperoxidase levels, and proinflammatory cytokine/chemokine levels (interleukin-1 β [IL-1 β], IL-6, IL-10, keratinocyte chemokine, macrophage inflammatory protein 1 α , macrophage inflammatory protein 1 β , and regulated upon activation normal T-cell expressed, secreted chemokine). Phenotypic analysis of lung cells showed an increase in T-cell numbers after TH. The vast majority of these cells were $\alpha\beta$ T cells, irrespective of injury. Although $\gamma\delta$ T cells were a small percentage of the total T-cell infiltrate, their numbers did increase after injury. In mice lacking $\gamma\delta$ T cells (δ TCR^{-/-} mice), TH-induced T-cell infiltration of the lung was markedly attenuated, whereas infiltration of other inflammatory cells was increased (i.e., monocytes, granulocytes, and myeloid-derived suppressor cells). In conclusion, these findings suggest that $\gamma\delta$ T cells regulated the infiltration of the lung with inflammatory cells after injury.

KEYWORDS—Injury, receptors, inflammation, cytokines

INTRODUCTION

After a traumatic injury, hemorrhage is responsible for more than 35% of prehospital deaths and more than 40% of deaths within first 24 h after injury (1). Acute lung injury (ALI) and acute respiratory distress syndrome are common complications and remain a major cause of morbidity and mortality under such conditions. Acute lung injury is caused by different local (pneumonia) or systemic (sepsis) inflammation. Activation of a proinflammatory cascade involving T cells, macrophages, and neutrophils play a major role in the pathogenesis of inflammatory mediator-induced lung injury from sepsis, pneumonia, and shock (2, 3).

Several studies have implicated T cells in the development and progression of different types of lung injuries. In humans, T cells are found in high abundance in lung biopsy specimens (4) and lavage fluid (5) in patients with pulmonary fibrosis, suggestive of their role during the injury process. However, most of these studies have focused on $\alpha\beta$ T cells. Recent evidence suggests that a unique T-cell subset, $\gamma\delta$ T cells, plays a pivotal role in the response to tissue injury (6). Gamma-delta T cells are involved in different disease processes, suggesting a role for this T-cell subset in both innate and acquired immunity (7, 8). Studies have shown that $\gamma\delta$ T cells are required for both controlled inflammatory and protective responses to direct pulmonary injury by infection or noxious agents (9, 10).

Clinical findings suggest the presence of activated $\gamma\delta$ T cells in the circulation of patients with SIRS (systemic inflammatory response syndrome) (11), which can also be associated with ALI. Furthermore, $\gamma\delta$ T cells are increased in response to bleomycin and attenuate the related lung fibrosis (12, 13). Nonetheless, it is unknown what role $\gamma\delta$ T cells play in the development of ALI after trauma-hemorrhage (TH).

MATERIALS AND METHODS

Mice

C57BL/6 (WT) and mice lacking $\gamma\delta$ T cells (δ TCR^{-/-}; C57BL/6 J-Tcrd^{tm1Mom}) male mice (30–35 g; the Jackson Laboratory, Bar Harbor, Maine) were used for all the experiments. The Tcrd^{tm1Mom}/Tcrd^{tm1Mom} (δ TCR^{-/-}) mice used for the study had the same initial target strain (C56BL/6 J) and backcross strain (C56BL/6 J). Mice were allowed to acclimatize for at least 1 week before experimentation and maintained in ventilated cages under specific pathogen-free conditions. Animals were randomly assigned into either sham or TH group. All animal protocols were approved by the Institutional Animal Care and Use Committee of the University of Texas Health Science Center at San Antonio and were performed in accordance with the National Institutes of Health guidelines for the care and handling of laboratory animals.

TH procedure

A fixed-volume TH model developed by Abraham and Freitas was used with modifications (14). Briefly, the mice were anesthetized by intramuscular injection of ketamine/xylazine. The abdomen was clipped, cleaned, and prepared for aseptic procedures. A 2-cm longitudinal incision was made along the midline to cause a soft tissue trauma. The intestine was placed on one side to expose the inferior vena cava. Approximately 30% (~0.55 mL for a 20-g mouse) of total blood volume was withdrawn during a 60-s period using a 27-gauge needle and syringe to induce hemorrhagic shock. The intestine was repositioned in the peritoneal cavity, and the peritoneal wall and the skin were closed in two layers with 5-0 nonabsorbable sutures. Ringer's lactate solution (three times the shed blood volume) was given intraperitoneally for resuscitation at 60 min after the surgery. Control (sham) animals were anesthetized, opened, and closed, with no blood being withdrawn. The cages were placed on a heating pad until sacrifice.

Lung tissue collection

At 2 h after resuscitation (3 h after surgery) in the TH group or 3 h after sham treatment, the lungs were perfused with ice-cold phosphate buffer solution (PBS)

Address reprint requests to Martin G. Schwacha, PhD, Department of Surgery, University of Texas Health Science Center at San Antonio, Mail Code 7740, 7703 Floyd Curl Dr, San Antonio TX 78229-3900. E-mail: schwacha@uthscsa.edu.

These findings were presented in part at the 34th annual meeting of the Shock Society in Norfolk, Virginia.

This work was supported by funding from the University of Texas Health Science Center at San Antonio Department of Surgery.

DOI: 10.1097/SHK.0000000000000358

Copyright © 2015 by the Shock Society

Report Documentation Page

*Form Approved
OMB No. 0704-0188*

Public reporting burden for the collection of information is estimated to average 1 hour per response, including the time for reviewing instructions, searching existing data sources, gathering and maintaining the data needed, and completing and reviewing the collection of information. Send comments regarding this burden estimate or any other aspect of this collection of information, including suggestions for reducing this burden, to Washington Headquarters Services, Directorate for Information Operations and Reports, 1215 Jefferson Davis Highway, Suite 1204, Arlington VA 22202-4302. Respondents should be aware that notwithstanding any other provision of law, no person shall be subject to a penalty for failing to comply with a collection of information if it does not display a currently valid OMB control number.

1. REPORT DATE 01 JUN 2015		2. REPORT TYPE N/A		3. DATES COVERED -	
4. TITLE AND SUBTITLE Gamma Delta T-Cells Regulate Inflammatory Cell Infiltration of the Lung after Trauma-Hemorrhage				5a. CONTRACT NUMBER	
				5b. GRANT NUMBER	
				5c. PROGRAM ELEMENT NUMBER	
6. AUTHOR(S) Rani, Meenakshi; Zhang, Qiong; Oppeltz, Richard F.; Schwacha, Martin G.;				5d. PROJECT NUMBER	
				5e. TASK NUMBER	
				5f. WORK UNIT NUMBER	
7. PERFORMING ORGANIZATION NAME(S) AND ADDRESS(ES) United States Army Institute of Surgical Research, JBSA Fort Sam Houston, TX 78234				8. PERFORMING ORGANIZATION REPORT NUMBER	
9. SPONSORING/MONITORING AGENCY NAME(S) AND ADDRESS(ES)				10. SPONSOR/MONITOR'S ACRONYM(S)	
				11. SPONSOR/MONITOR'S REPORT NUMBER(S)	
12. DISTRIBUTION/AVAILABILITY STATEMENT Approved for public release, distribution unlimited					
13. SUPPLEMENTARY NOTES					
14. ABSTRACT					
15. SUBJECT TERMS					
16. SECURITY CLASSIFICATION OF:			17. LIMITATION OF ABSTRACT SAR	18. NUMBER OF PAGES 9	19a. NAME OF RESPONSIBLE PERSON
a. REPORT unclassified	b. ABSTRACT unclassified	c. THIS PAGE unclassified			

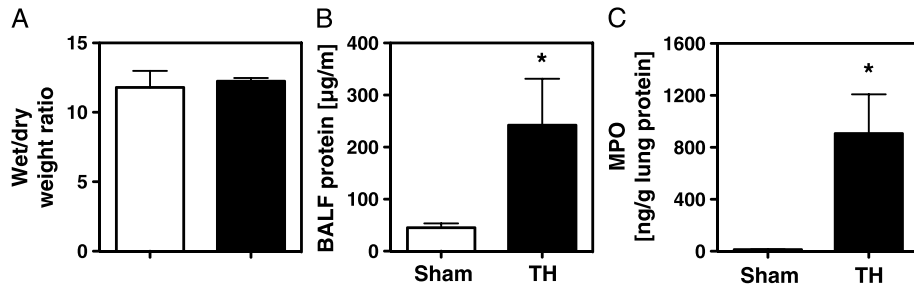


FIG. 1. **TH is associated with ALI.** Lungs from WT mice were harvested after 2 h of injury or sham procedure and used to assay wet/dry weight ratio, lung permeability, and MPO contents as described in the Materials and Methods section. A, Wet/dry weight ratio. B, Lung permeability after TH as determined by the BALF protein concentrations. C, The MPO activity after TH. Data are expressed as mean \pm SEM for 4 to 12 mice per group. * P < 0.05 vs. respective sham group.

to eliminate circulating blood. After perfusion, the lungs were removed and the left lobe was immediately snap frozen in liquid nitrogen and stored at -80°C for the determination of myeloperoxidase (MPO) activity and cytokine/chemokine analysis. The right lung was used to isolate single cells for flow cytometry.

Lung lysate preparation and protein determination

Lungs from -80°C were thawed and homogenized in homogenization buffer containing protease inhibitor cocktail (Calbiochem, San Diego, Calif). The tissue extract was clarified by centrifugation at 14,000 rpm for 20 min. Lysate protein concentration was determined using a Bio-Rad protein assay (Bio-Rad Laboratories, Hercules, Calif) and used for cytokine/chemokine analyses.

Lung digestion and single-cell isolation

Right lung lobes were removed and rinsed with PBS. Lungs were placed into 10 mL of RPMI containing 0.2% collagenase (LS004196; Worthington, Lakewood, NJ) and 50 units DNase I (D4263; Sigma Chemical, St. Louis, Mo). The lungs were cut into small pieces and digested at 37°C for 30 min with intermittent shaking every 5 min. The digested lungs were then passed through a 100- μm mesh-size nylon mesh and centrifuged at 400g for 10 min at 4°C . The cell pellet was resuspended in Gey solution (NH_4Cl and KHCO_3 buffer) for 5 min to lyse red blood cells. Isolated single cells were counted and used for flow cytometry.

Lung wet/dry weight ratio

To determine the lung edema, the lung wet/dry weight was calculated. The upper lobe of the right lung was excised, and the wet weight was recorded. The lung was then dried at room temperature for 48 h until a stable dry weight is achieved, and the wet/dry weight ratios were calculated.

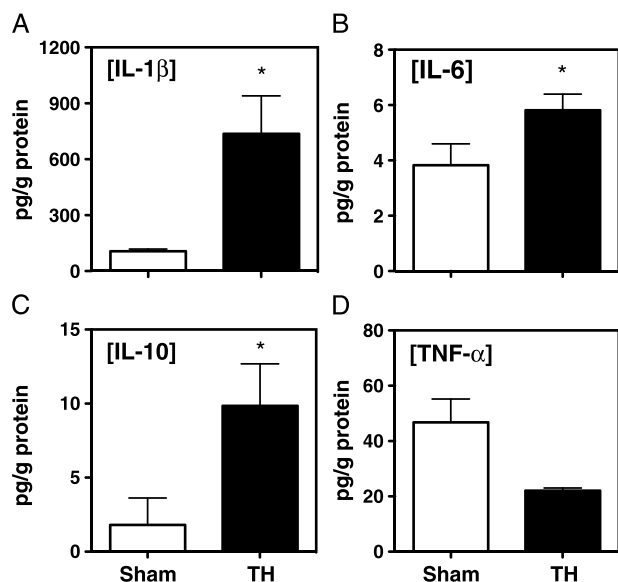


FIG. 2. **Inflammatory cytokine production by lung cells after TH.** Lung tissues from WT mice were removed at 2 h after TH or sham procedure. Lung lysates were prepared as described in the Materials and Methods section and used for cytokine analyses. The IL-1 β (A), IL-6 (B), IL-10 (C), and TNF- α (D) levels were determined by Bioplex (Bio-Rad). Data are expressed as mean \pm SEM for three mice per group. * P < 0.05 vs. respective sham group.

Lung permeability

Changes in lung permeability were determined by collection of bronchoalveolar lavage fluid (BALF) to assess protein concentration as an index of lung permeability (injury) (15).

MPO activity

Lung lysates were assayed for MPO activity with enzyme-linked immunosorbent assay kits (Hycult Biotech). All procedures were carried out in accordance with the manufacturer's instructions. Myeloperoxidase levels in the lung samples were normalized to milligrams of total protein.

Cellular phenotyping by flow cytometry

The lung cells were washed in staining buffer (PBS with 0.2% bovine serum albumin and 0.09% NaN_3) and treated with Fc-blocking antibody (anti-CD16/CD32; BD Biosciences) for 15 min. The cells were then stained with the following

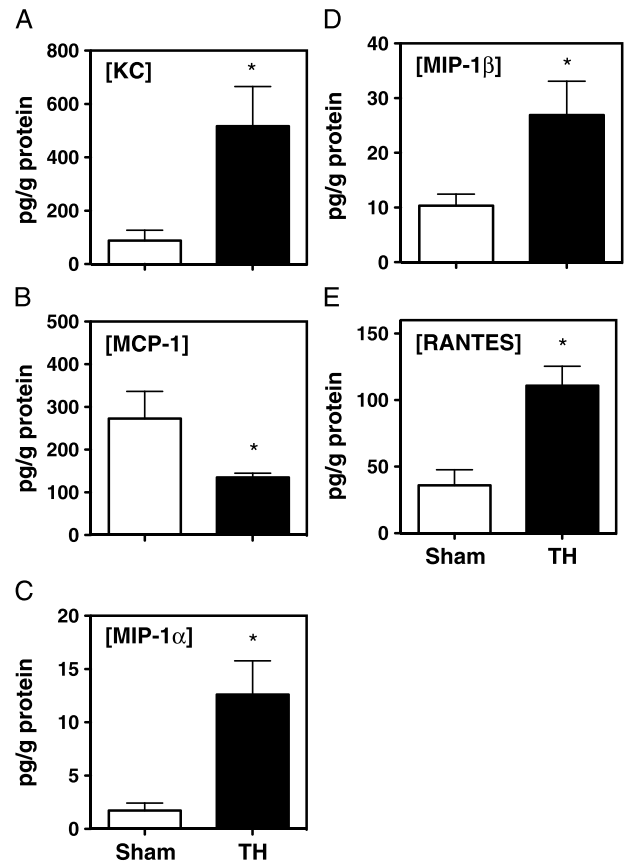


FIG. 3. **Chemokine production by lung cells at 2 h after TH.** Lung tissues from WT mice were removed at 2 h after TH or sham procedure. Lung lysates were prepared as described in the Materials and Methods section and used for cytokine analyses. The keratinocyte chemokine (KC) (A), MCP-1 (B), MIP-1 α (C), MIP-1 β (D), and RANTES (E) levels were determined by Bioplex (Bio-Rad). Data are expressed as mean \pm SEM for three mice per group. * P < 0.05 vs. respective sham group.

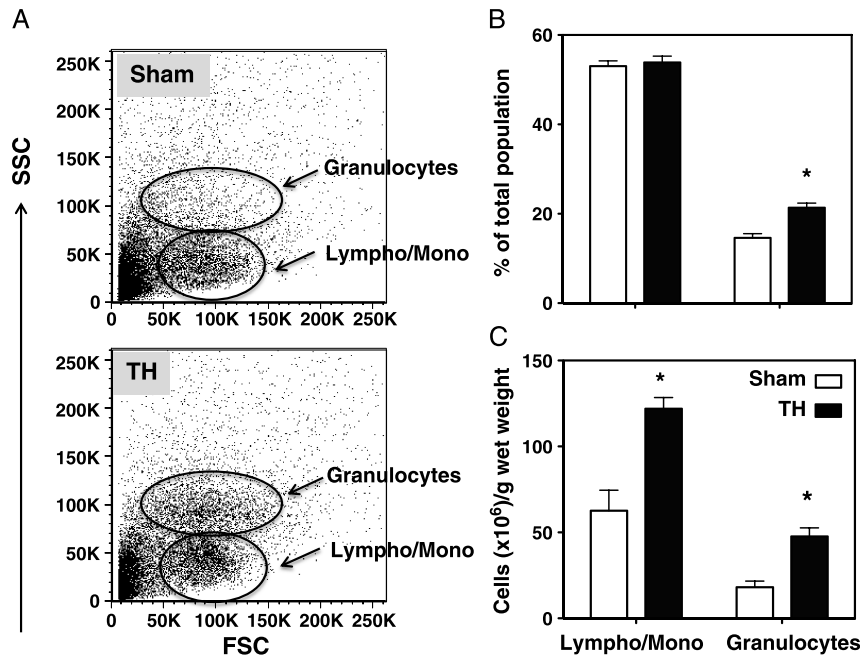


FIG. 4. **Effect of TH on lung cell populations.** At 2 h of injury or sham procedure, lung single cells from WT mice were prepared using collagenase/DNAse digestion and used for flow cytometry. A, The lymphocyte/monocyte (Lympho/Mono) and granulocyte populations were identified by forward (FSC) and side scatter (SSC), as shown in the representative dot blots. B, The populations were analyzed as percentages of the total viable cell populations. Data are expressed as mean \pm SEM for 9 to 11 mice per group. * $P < 0.05$ vs. respective sham group.

directly conjugated antibodies: anti-CD3 (PE or APC-Cy7) in combination with anti- β TCR (PerCPCy5.5), anti- γ TCR (FITC), anti-CD4 (APC), anti-CD8 (APC-Cy7), anti-CD11b (PerCPCy5.5), and Gr1 (Ly6G; Pacific Blue). After 30 min on ice, the cells were washed and resuspended in staining buffer. Appropriate isotype controls were used for all staining. All data were acquired using an LSRII (BD Biosciences) and analyzed using FlowJo software (FlowJo, Treestar). A minimum of 50,000 events was collected, and live cells were gated according to forward and side scatter properties. Total cell number was calculated as percentage cells \times total number of cells per gram wet weight of lung/100.

Analysis of cytokines and chemokine levels

Lung lysates were analyzed for cytokine/chemokine levels (interleukin-1 β [IL-1 β], IL-6, IL-10, tumor necrosis factor- α [TNF- α], keratinocyte chemokine (KC), monocyte chemoattractant protein 1 [MCP-1], macrophage inflammatory protein 1 α [MIP-1 α], MIP-1 β , and regulated upon activation normal T-cell expressed, secreted chemokine [RANTES]), by Bioplex (Bio-Rad) according to the manufacturer's recommendations. Cytokine levels were normalized to total protein levels of lung that were determined by BioRad protein assay as described earlier.

Statistical analyses

Data are expressed as mean \pm SEM. Comparisons were analyzed using analysis of variance, and Student *t* test was used for comparisons between two groups. A value of $P < 0.05$ was considered to be statistically significant for all analyses.

RESULTS

TH induces ALI

The development of ALI after TH was assessed by measuring changes in wet/dry weight ratio, lung permeability (BALF protein content), and neutrophil accumulation (MPO activity). At 2 h after TH, ALI was evident, with a significant increase in lung permeability and MPO accumulation (Fig. 1). Although wet/dry weight ratio remained comparable between the sham and TH groups (Fig. 1A), approximately a 5-fold increase in BALF protein levels was observed in TH mice as compared with shams (Fig. 1B). This change in lung permeability after TH was paralleled by a profound increase in MPO activity in the lung tissue, which was increased approximately 70-fold after TH as compared with lungs from sham mice (Fig. 1C).

TH induces a pulmonary inflammatory response

Trauma-hemorrhage-induced ALI was associated with increased levels of cytokines and chemokines in the lung tissue (Figs. 2 and 3). A profound increase in inflammatory cytokines such as IL-1 β , IL-6, and IL-10 was observed in lung tissues of TH mice as compared with shams (Fig. 2, A–C, respectively). Interleukin-1 β , IL-6, and IL-10 levels were up to 7-fold greater in the TH mice as compared with those of sham mice. In contrast, TNF- α levels were lower (2-fold) in TH mice when compared with those in sham mice (Fig. 2D).

Similar to cytokines, the levels of chemokines (i.e., KC, MIP-1 α , MIP-1 β , and RANTES) were also increased after TH as compared with those in shams (Fig. 3). Although the levels of KC and MIP-1 α were more than 5-fold greater (Fig. 3, A and C), MIP-1 β and RANTES were increased by approximately 2-fold (Fig. 3, D and E) in TH mice. On the contrary, MCP-1 levels were lower (2-fold) in TH mice when compared with those in sham mice (Fig. 3B).

TH-induced changes in pulmonary immune cells

After TH, a profound change in the phenotype of lung immune cells isolated after lung digestion was observed (Fig. 4). An approximately 2-fold increase in total number of viable cells per gram of lung wet weight was observed after TH as compared with sham treatment (Table 1). For phenotypic analysis of different immune cells, lymphocyte/monocyte (Lymph/Mono)

TABLE 1. **Impact of TH on total lung cells**

	Cells (10 ⁶)/g wet weight
Sham	39.81 \pm 4.3*
TH	75.26 \pm 4.7 [†]

*Data are expressed as mean \pm SEM (n = 5 mice per group).

[†] $P < 0.05$ vs. sham.

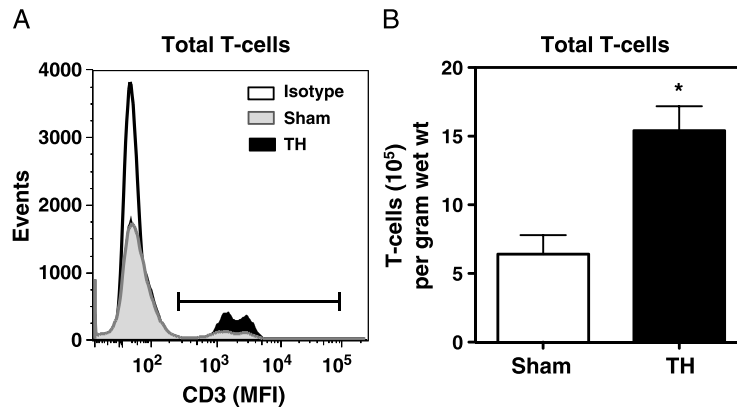


FIG. 5. **Effect of TH on total T-cell population.** Lung cells from WT mice were prepared after 2 h of injury or sham procedure and studied for total T-cell phenotype by flow cytometry. Cells were stained with anti-CD3 to identify total T cells. A, Representative histogram overlays for CD3 cells, gated on lympho/mono population, for isotype, sham, and TH mice. B, Number of total T cells per gram wet weight of tissue. Data are mean \pm SEM for four to five mice per group. * $P < 0.05$ vs. sham group.

and granulocyte populations were identified based on their forward and side scatter properties as shown in Figure 4A. Although the percentage of lymphocytes/monocytes was comparable between sham and TH mice (Fig. 4B), a significant increase in the percentage of granulocytes in the lung of TH mice was evident (Fig. 4B). However, when cell percentages were normalized to gram wet weight, a significant increase (2-fold for lymphocytes/monocytes; 3-fold for granulocytes) in the numbers of both lymphocytes/monocytes and granulocytes after TH was observed as compared with sham skin, which was significantly greater than that observed in sham mice (Fig. 4C).

TH alters lung T-cell populations

A profound influx of total T cells was observed after TH (Fig. 5). Both the percentage and absolute numbers for CD3⁺

total T cells were significantly increased after TH in comparison with the T-cell percentages and numbers in lung cells from sham mice (Fig. 5, A and B).

Lung cells were stained with anti-CD3 in combination with δ TCR and β TCR antibodies to characterize $\gamma\delta$ T cells (Fig. 6, A and B) and $\alpha\beta$ T cells (Fig. 6, C and D), respectively. Characterization of T cells demonstrated that the vast majority of T cells were positive for $\alpha\beta$ TCR (~90%–95%) after TH (Fig. 6, A and B). Both the percentages and numbers of $\alpha\beta$ T cells were increased after TH as compared with the sham group (Fig. 6, A and B). In contrast, $\gamma\delta$ T cells contributed to a small percentage of the total T cells (~5%–10%); however, similar to $\alpha\beta$ T cells, their percentage (Fig. 6C) as well as absolute number (Fig. 6D) increased significantly after TH.

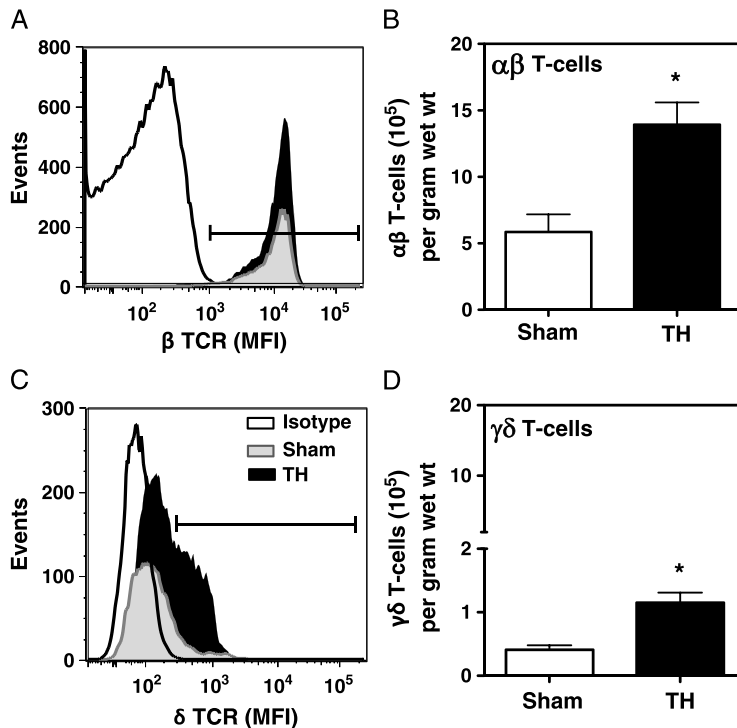


FIG. 6. **Effect of TH on $\gamma\delta$ and $\alpha\beta$ T-cell populations.** Lung cells from WT mice were prepared after 2 h of injury or sham procedure and studied for $\gamma\delta$ and $\alpha\beta$ T-cell phenotype by flow cytometry. Cells were stained with anti-CD3 in combination with anti- β TCR or anti- δ TCR antibody to identify $\alpha\beta$ T cells or $\gamma\delta$ T cells, respectively. Panels A and C show representative histogram overlays for $\gamma\delta$ and $\alpha\beta$ T cells, respectively, gated on CD3⁺ total T cells, for isotype, sham, and TH mice. Panels B and D show the number of $\gamma\delta$ and $\alpha\beta$ T cells, respectively per gram wet weight of tissue. Data are mean \pm SEM for four to five mice per group. * $P < 0.05$ vs. sham group.

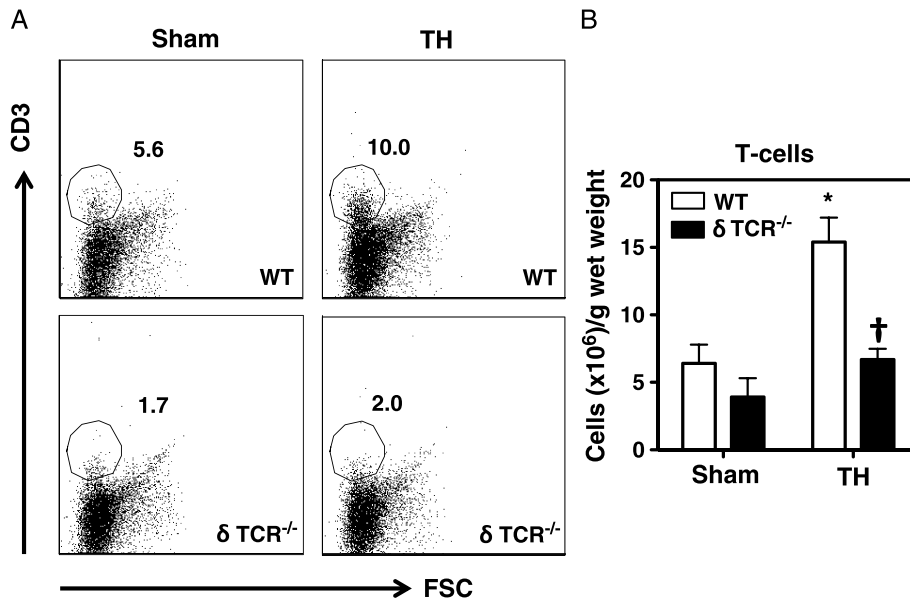


FIG. 7. **Effect of $\gamma\delta$ T cells on infiltrating CD3 T cells.** Lung cells from WT or δ TCR^{-/-} mice were prepared after 2 h of injury or sham procedure and analyzed for T-cell phenotype by flow cytometry as described in the Materials and Methods section. A, Representative data for all CD3⁺ cells. B, Cumulative data (in percent) for T cells. Data are mean \pm SEM for three to five mice per group. **P* < 0.05 vs. respective sham group. †*P* < 0.05 vs. TH group from WT mice.

Alpha-beta T cells were further investigated in terms of the CD4 and CD8 surface expression (Table 2), and the following subsets were identified: CD4⁻CD8⁻ double-negative, CD4⁺CD8⁻ (CD4-positive $\alpha\beta$ T cells), CD4⁻CD8⁺ (CD8-positive $\alpha\beta$ T cells), and double-positive CD4⁺CD8⁺ $\alpha\beta$ T cells. Although majority of the $\alpha\beta$ T cells belonged to either CD4⁺ (~41% – 43%) or CD8⁺ (~53% – 56%) subsets irrespective of the injury, a very small percentage of $\alpha\beta$ T cells were either double negative (CD4⁻CD8⁻; 1.5% – 2.0%) or double positive (CD4⁺CD8⁺; ~1.7%). After TH, the percentage of these CD4 and CD8 subsets was comparable to that of sham group except for single-positive $\alpha\beta$ T cells that was significantly increased after TH (Table 2).

$\gamma\delta$ T cells regulate lung infiltration after TH

The impact of $\gamma\delta$ T cells on TH-induced ALI was investigated through the use of mice deficient in $\gamma\delta$ T cells. A profound attenuation in the TH-induced infiltration of the lung with T cells was observed in the mice lacking $\gamma\delta$ T cells (δ TCR^{-/-} mice) in comparison with that observed in WT mice (Fig. 7). Further analysis of the T cells infiltrating the lung showed a similar pattern for $\alpha\beta$ T cells (data not shown). The numbers of T cells in δ TCR^{-/-} mice were increased marginally after TH (Fig. 7); however, the numbers of these T cells was reduced by 80% after TH as compared with those in WT mice (Fig. 7).

The impact of $\gamma\delta$ T cells on other lung inflammatory cells was also evaluated, as shown in Figures 8 to 10. Trauma-hemorrhage

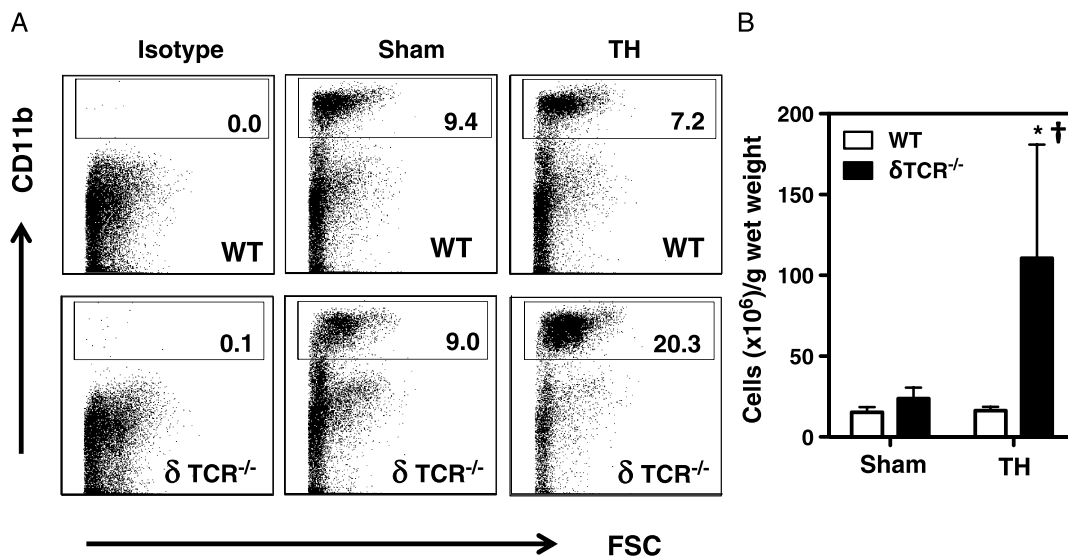


FIG. 8. **Effect of $\gamma\delta$ T cells on monocyte populations.** Lung cells from WT or δ TCR^{-/-} mice were prepared after 2 h of injury or sham procedure and studied for CD11b⁺ monocytes using flow cytometry. A, Gating strategy. CD11b⁺ cells from the lympho/mono cell gate of WT (Fig. 8A, upper panel) and δ TCR^{-/-} (Fig. 8A, lower panel) mice. Representative dot plots are shown from sham and TH mice from both WT and δ TCR^{-/-} mice. The numbers indicate the percentages of CD11b⁺ cells as determined by flow cytometry. B, The number of CD11b⁺ cells as normalized to gram of wet weight of lung tissue. Data are mean \pm SEM for three to five mice per group. **P* < 0.05 vs. respective sham group. †*P* < 0.05 vs. TH group from WT mice.

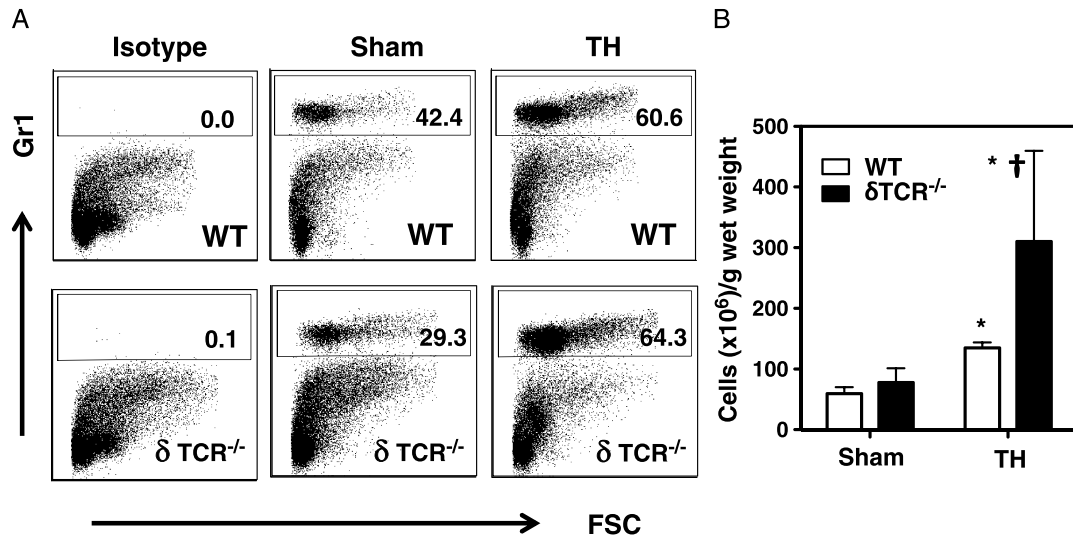


FIG. 9. **Effect of $\gamma\delta$ T cells on granulocyte populations.** Lung cells from WT or δ TCR^{-/-} mice were prepared after 2 h of injury or sham procedure and studied for Gr1⁺ granulocytes using flow cytometry. A, Gating strategy. Gr1⁺ cells from the lympho/mono cell gate of WT (Fig. 9A, upper panel) and δ TCR^{-/-} (Fig. 9A, lower panel) mice. Representative dot plots are shown from sham and TH mice from both WT and δ TCR^{-/-} mice. The numbers indicate the percentages of respective population as determined by flow cytometry. B, The number of Gr1⁺ cells as normalized to gram of wet weight of lung tissue. Data are mean \pm SEM for three to five mice per group. * $P < 0.05$ vs. respective sham group. † $P < 0.05$ vs. TH group from WT mice.

induced a significant infiltration of the lung with monocytes (Fig. 8), neutrophils (Fig. 9), and myeloid-derived suppressor cells (MDSCs) (Fig. 10) in both WT and δ TCR^{-/-} mice; however, the degree of the infiltration of the inflammatory cells was significantly greater in the lungs of δ TCR^{-/-} mice after TH. The numbers for monocytes were increased significantly after injury in δ TCR^{-/-} mice, whereas they remained unchanged in WT group (Fig. 8). Along with the percentages and absolute numbers, the data were further analyzed for median fluorescence intensity of CD11b⁺ as an indicator of activation. The median fluorescence intensity of CD11b⁺ cells was increased marginally but not significantly increased after TH in both WT (51,758 \pm 1,157 for sham vs. 55,0051 \pm 1,361 for TH) and δ TCR^{-/-} (43,485 \pm 4,173 for sham vs. 48,955 \pm 3,541 for TH) mice. Comparison of the WT mice with δ TCR^{-/-} mice did not show a significant difference, irrespective of TH. The

numbers of granulocytes after injury were increased in both WT and δ TCR^{-/-} mice when compared with their respective sham groups (Fig. 9). However, this increase in granulocyte population was many folds higher in the δ TCR^{-/-} group compared with that in the WT group (Fig. 9). Further analysis of myeloid cells revealed that MDSCs (i.e., CD11b⁺Gr1⁺ cells), just like granulocytes, were increased after TH in both WT and δ TCR^{-/-} mice (Fig. 10). However, the increase was almost four times greater in the δ TCR^{-/-} group.

The impact of $\gamma\delta$ T cells on the development of ALI after TH was assessed (Tables 3 – 5). The lack of $\gamma\delta$ T cells did not alter the TH-induced increases in markers of ALI, such as wet/dry weight ratio, lung permeability (BALF protein content), and polymorphonuclear leukocyte (PMN) accumulation (MPO activity) (Table 2). With regard to the inflammatory response, the basal level of all the cytokines and chemokines from

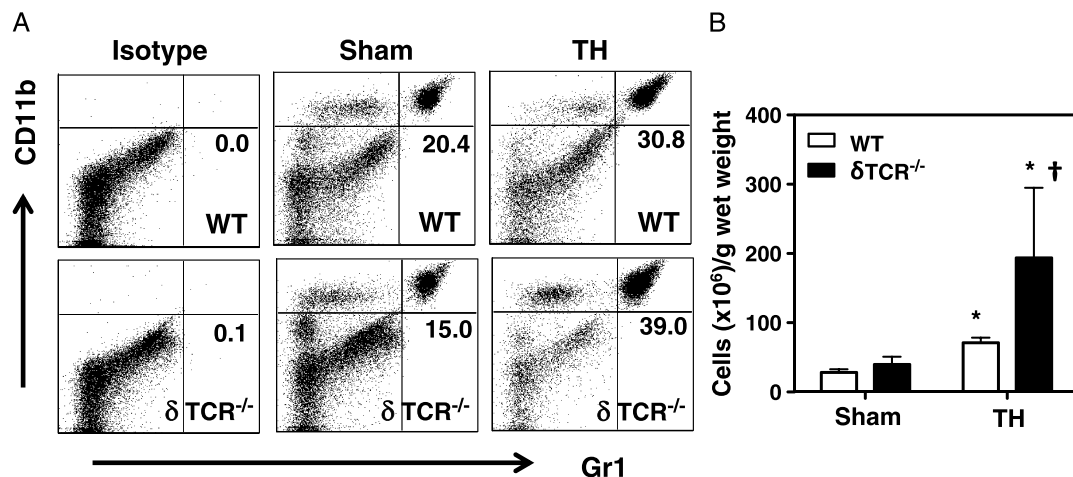


FIG. 10. **Impact of $\gamma\delta$ T cells on MDSCs.** Lung cells from WT or δ TCR^{-/-} mice were prepared after 2 h of injury or sham procedure and studied for CD11b⁺Gr1⁺ MDSCs using flow cytometry. A, Gating strategy. CD11b⁺Gr1⁺ cells from the lympho/mono cell gate of WT (Fig. 10A, upper panel) and δ TCR^{-/-} (Fig. 10A, lower panel) mice. Representative dot plots are shown from sham and TH mice from both WT and δ TCR^{-/-} mice. The numbers indicate the percentages of respective population as determined by flow cytometry. B, The number of CD11b⁺Gr1⁺ cells as normalized to gram of wet weight of lung tissue. Data are mean \pm SEM for three to five mice per group. * $P < 0.05$ vs. respective sham group. † $P < 0.05$ vs. TH group from WT mice.

TABLE 2. CD4 and CD8 expression on $\alpha\beta$ T cells

	CD4 ⁻ CD8 ⁻	CD4 ⁻ CD8 ⁺	CD4 ⁺ CD8 ⁻	CD4 ⁺ CD8 ⁺
Sham	1.5 ± 0.1*	41.4 ± 1.1	55.5 ± 1.1	1.7 ± 0.1
TH	2.4 ± 0.2 [†]	43.4 ± 1.2	52.5 ± 1.2	1.7 ± 0.1

*Data are expressed as mean percentage expression ± SEM (n = 15 mice per group).

[†]P < 0.05 vs. respective sham group.

Lungs from WT mice were harvested after 2 h of injury or sham procedure and analyzed for CD4 and CD8 expression on $\alpha\beta$ T cells as described in the Materials and Methods section. The numbers represent the cumulative data (in percent) for CD4 or CD8 subsets of $\alpha\beta$ T cells.

sham mice of δ TCR^{-/-} mice was increased profoundly when compared with sham of the WT mice (Tables 3 and 4). An increase in inflammatory cytokines such as IL-1 β and IL-6 in δ TCR^{-/-} mice after TH was found comparable to that in WT mice (Fig. 2, A – C; Table 4). Tumor necrosis factor- α levels were decreased after TH in both WT and δ TCR^{-/-} mice. Although IL-10 levels significantly increased after TH in WT mice, the levels of IL-10 cytokine were decreased after TH in δ TCR^{-/-} mice (Table 4). Regarding chemokines, the levels of KC, MIP-1 β , and RANTES that were significantly increased after TH in WT mice (Fig. 3) either remained comparable (KC) or were decreased (MIP-1 β and RANTES) after TH in δ TCR^{-/-} mice (Table 5). The MIP-1 α was increased after TH in WT mice and remained significantly increased after TH in δ TCR^{-/-} mice also. Although MCP-1 levels significantly decreased after TH in WT mice, the levels of MCP were significantly increased after TH in δ TCR^{-/-} mice (Table 5).

DISCUSSION

The studies presented here were conducted to determine the role of $\gamma\delta$ T cells in response to TH-induced ALI. We document here a number of important findings regarding the regulatory role of $\gamma\delta$ T cells in the infiltration of T cells and myeloid cells into lung after TH. First, we observed that TH induced ALI, which was associated with a profound increase in the pulmonary immune cell populations, as well as significantly elevated levels of a number of inflammatory cytokines/chemokines. Second, after TH, $\gamma\delta$ T cells are important in the infiltration of the lung with $\alpha\beta$ T cells because, in the absence of $\gamma\delta$ T cells, a profound decrease of $\alpha\beta$ T-cell infiltration was observed. Third, the infiltration of myeloid cells was also $\gamma\delta$ T cell dependent. Analysis of myeloid cells revealed that the infiltration of MDSCs was significantly increased in δ TCR^{-/-} mice. We propose that resident $\gamma\delta$ T cells regulate the influx of $\alpha\beta$ T cells and MDSCs,

TABLE 4. Impact of $\gamma\delta$ T cells on lung cytokine levels (pg/g of lung protein)

	WT		δ TCR ^{-/-}	
	Sham	TH	Sham	TH
IL-1 β	107 ± 11*	737 ± 203 [†]	955 ± 202	1773 ± 567 [†]
IL-6	4 ± 1	6 ± 1 [†]	12 ± 0.4	20 ± 6
IL-10	2 ± 2	10 ± 3 [†]	243 ± 48	184 ± 31
TNF- α	47 ± 8	22 ± 1 [†]	449 ± 51	311 ± 24

*Data are expressed as mean picograms per gram protein ± SEM (n = 3 – 12 mice per group).

[†]P < 0.05 vs. respective sham group.

Lungs from WT or δ TCR^{-/-} mice were harvested at 2 h after injury or sham procedure and analyzed for cytokines as described in the Materials and Methods section. WT cytokine data are presented in Figure 2 and shown here for comparative purposes.

which are the primary effector cells of the inflammatory and healing responses.

Acute lung injury and acute respiratory distress syndrome are common complications after TH and induce a profound immunoinflammatory response that may lead to the development of multiple organ failure and ultimately death. Susceptibility to lung neutrophil accumulation and local tissue cytokine/chemokine increase is shown to be associated with lung injury after hemorrhagic shock (16, 17). Consistent with the current literature, our TH model was associated with ALI with increased lung permeability, neutrophil influx, and elevated levels of inflammatory cytokines (IL-1 β , IL-6, IL-10) and chemokines (KC, MIP-1 α , MIP-1 β , and RANTES).

Our current findings demonstrate that the majority of T cells in mouse lung are $\alpha\beta$ T cells, and $\gamma\delta$ T cells make a very small number of the total T-cell population. The total number of total T cells in the lung was significantly increased after TH, which is caused by increase in both $\alpha\beta$ and $\gamma\delta$ T cells after injury. It can be speculated that the tissue damage causes migration of different immune cells into the circulation and then to the site of injury to help control inflammation. Previous studies on other pathological conditions support this concept (18, 19). Li et al. (20) in a corneal epithelial mouse model have also shown an increase in the number of $\gamma\delta$ T cells at the injury site within 24 h. They demonstrated the accumulation of $\gamma\delta$ T cells in the corneal epithelium within 18 h after injury and remained at elevated levels for at least 7 days (21). Purcell et al. (22) have shown that burn injury causes CD4 T-cell proliferation in the lymph nodes draining from the injury site, which is in line with our current finding (23).

TABLE 3. Impact of $\gamma\delta$ T cells on the markers of ALI

	WT		δ TCR ^{-/-}	
	Sham	TH	Sham	TH
Wet/dry weight ratio	11.8 ± 1.2	12.2 ± 0.2	11.1 ± 1.8	16.4 ± 1.9
Lung permeability (μ g of protein/mL BALF)	430.6 ± 44.2*	684.73 ± 63.4 [†]	388.6 ± 19.3	556.81 ± 9.8 [†]
PMN accumulation (MPO content; ng/g lung protein)	13.4 ± 1.4	907.2 ± 302.0 [†]	22.25 ± 3.2	1133.1 ± 67.4 [†]

*Data are expressed as mean ± SEM (n = 3 – 12 mice per group).

[†]P < 0.05 vs. respective sham group.

Lungs from WT or δ TCR^{-/-} mice were harvested after 2 h of injury or sham procedure and analyzed for the markers of ALI. Wet/dry weight ratio, lung permeability, and PMN accumulation were determined as described in the Materials and Methods section.

TABLE 5. Impact of $\gamma\delta$ T cells on lung chemokine levels (pg/g of lung protein)

	WT		δ TCR ^{-/-}	
	Sham	TH	Sham	TH
KC	88 ± 39*	517 ± 149 [†]	22 ± 3	28 ± 3
MCP-1	273 ± 64	135 ± 10 [†]	1,066 ± 221	2,161 ± 399 [†]
MIP-1 α	2 ± 1	13 ± 3 [†]	1 ± 1	4 ± 3 [†]
MIP-1 β	10 ± 2	27 ± 6 [†]	526 ± 250	332 ± 79
RANTES	36 ± 12	111 ± 15 [†]	214 ± 125	123 ± 28

*Data are expressed as mean picograms per gram protein ± SEM (n = 3–12 mice per group).

[†]P < 0.05 vs. respective sham group.

Lungs from WT or δ TCR^{-/-} mice were harvested at 2 h after injury or sham procedure and analyzed for chemokines as described in the Materials and Methods section. WT chemokine data have also been presented in Figure 3 and shown here for comparative purposes.

We observed a significantly increased infiltration of both lymphoid and myeloid cells in WT mice after TH-induced ALI. In parallel to $\gamma\delta$ T cells, myeloid cells (i.e., monocytes, PMNs, and MDSCs) were also increased significantly after the injury. A growing body of literature demonstrates the influx of myeloid cells, especially MDSCs, after injury, inflammation, and infection consistent with the finding herein. Our findings confirmed previous reports demonstrating the increased neutrophils during ALI (24). Regarding trauma, Makarenkova and others in a mouse model have demonstrated the infiltration of MDSCs into the spleen after injury (25, 26). In addition, in a burn injury model, we and others demonstrated increased myeloid cells such as monocytes and MDSCs at the wound site after burn injury (27, 28).

In the present study, we demonstrated that, in the absence $\gamma\delta$ T cells, the numbers of leukocytes increased in the lungs after TH. It could be speculated that the tissue damage causes migration of immune cells into the circulation and to the site of injury where they play a role in regulating the inflammatory response. However, in δ TCR^{-/-} mice, the markers of ALI, that is, wet/dry ratio, BALF protein leakage, and MPO levels, did not change after TH when compared with those of WT animals. This lack of an effect may be related to injury severity. Importantly, the presence of both $\alpha\beta$ T cells and myeloid cells in the lung after TH was $\gamma\delta$ T cell dependent. Although $\alpha\beta$ T cells were virtually absent in mice lacking $\gamma\delta$ T cells, the influx of myeloid cells was further elevated. The increase in myeloid cells in δ TCR^{-/-} mice supports the concept that $\gamma\delta$ T cells inhibited the influx of $\alpha\beta$ T cells that act to suppress the myeloid cells.

It is well established that $\gamma\delta$ T cells express chemokine receptor on their surfaces that help immune cells migrate to the site of injury or inflammation (29, 30). In addition, $\gamma\delta$ T cells can also produce chemokines such as RANTES and hence contribute to the recruitment of various inflammatory cells. The migration of CD8⁺ $\alpha\beta$ T cells to a wound has been shown to be induced by activated $\gamma\delta$ T cells (29). In contrast to the findings herein, Jameson et al. (30) have shown that $\gamma\delta$ T cells are essential in the rapid migration of macrophages to the wound site in a murine punch wound model. We speculate that these differences between our study and Jameson et al. (30)

may be in part related to the type of cells (PMNs, monocytes, and MDSCs versus macrophages), injury type (burn injury versus TH), and the overall course of inflammatory response during burn injury versus TH-induced ALI.

Our findings herein show a correlative relationship between $\gamma\delta$ T cells and lung infiltration by lymphocytes and leukocytes after TH. Although it is tempting to speculate that a causative relationship exists, this will need to be borne out in future studies directly examining the relationships between ALI, chemokines, cellular infiltration, and lung $\gamma\delta$ T cells.

In conclusion, the current findings demonstrate that TH induces ALI. Gamma-delta T cells regulate the myeloid cell recruitment into the lung directly or by limiting the infiltration of the $\alpha\beta$ T cells and seem to be overall protective to the host—most likely via regulation of inflammation. Nonetheless, additional studies are needed to develop a more comprehensive understanding of this unique T-cell subset and their role in postinjury lung immunopathology.

REFERENCES

- Kauvar DS, Lefering R, Wade CE: Impact of hemorrhage on trauma outcome: an overview of epidemiology, clinical presentations, and therapeutic considerations. *J Trauma* 60(6 Suppl):S3–S11, 2006.
- Angele MK, Knöferl MW, Schwacha MG, Ayala A, Bland KI, Cioffi WG, Josephson SL, Chaudry IH: Hemorrhage decreases macrophage inflammatory protein 2 and interleukin-6 release: a possible mechanism for increased wound infection. *Ann Surg* 229(5):651–660; discussion 660–661, 1999.
- Hawwa RL, Hokenson MA, Wang Y, Huang Z, Sharma S, Sanchez-Esteban J: IL-10 inhibits inflammatory cytokines released by fetal mouse lung fibroblasts exposed to mechanical stretch. *Pediatr Pulmonol* 46(7):640–649, 2011.
- Katzenstein AL, Zisman DA, Litzky LA, Nguyen BT, Kotloff RM: Usual interstitial pneumonia: histologic study of biopsy and explant specimens. *Am J Surg Pathol* 26(12):1567–1577, 2002.
- Costabel U, Guzman J: Bronchoalveolar lavage in interstitial lung disease. *Curr Opin Pulm Med* 7(5):255–261, 2001.
- Alexander M, Daniel T, Chaudry IH, Choudhry MA, Schwacha MG: T cells of the gammadelta T-cell receptor lineage play an important role in the postburn wound healing process. *J Burn Care Res* 27(1):18–25, 2006.
- MacLeod AS, Hemmers S, Garijo O, Chabod M, Mowen K, Witherden DA, Havran WL: Dendritic epidermal T cells regulate skin antimicrobial barrier function. *J Clin Invest* 123(10):4364–4374, 2013.
- Bonneville M, O'Brien RL, Born WK: Gammadelta T cell effector functions: a blend of innate programming and acquired plasticity. *Nat Rev Immunol* 10(7):467–478, 2010.
- King DP, Hyde DM, Jackson KA, Novosad DM, Ellis TN, Putney L, Stovall MY, Van Winkle LS, Beaman BL, Ferrick DA: Cutting edge: protective response to pulmonary injury requires gamma delta T lymphocytes. *J Immunol* 162(9):5033–5036, 1999.
- Braun RK, Ferrick C, Neubauer P, Sjoding M, Sterner-Kock A, Kock M, Putney L, Ferrick DA, Hyde DM, Love RB: IL-17 producing gammadelta T cells are required for a controlled inflammatory response after bleomycin-induced lung injury. *Inflammation* 31(3):167–179, 2008.
- Matsushima A, Ogura H, Fujita K, Koh T, Tanaka H, Sumi Y, Yoshiya K, Hosotsubo H, Kuwagata Y, Shimazu T, et al.: Early activation of gammadelta T lymphocytes in patients with severe systemic inflammatory response syndrome. *Shock* 22(1):11–15, 2004.
- Lo Re S, Dumoutier L, Couillin I, Van Vyve C, Yakoub Y, Uwambayinema F, Marien B, van der Brule S, Van Snieck J, Uyttenhove C, et al.: IL-17a-producing gammadelta T and Th17 lymphocytes mediate lung inflammation but not fibrosis in experimental silicosis. *J Immunol* 184(11):6367–6377, 2010.
- Pociask DA, Chen K, Choi SM, Oury TD, Steele C, Kolls JK: $\gamma\delta$ T cells attenuate bleomycin-induced fibrosis through the production of CXCL10. *Am J Pathol* 178(3):1167–1176, 2011.
- Abraham E, Freitas AA: Hemorrhage in mice induces alterations in immunoglobulin-secreting B cells. *Crit Care Med* 17(10):1015–1019, 1989.
- Kenyon NJ, van der Vliet A, Schock BC, Okamoto T, McGrew GM, Last JA: Susceptibility to ozone-induced acute lung injury in iNOS-deficient mice. *Am J Physiol Lung Cell Mol Physiol* 282(3):L540–L545, 2002.
- Ayala A, Chung CS, Lomas JL, Song GY, Doughty LA, Gregory SH, Cioffi WG, LeBlanc BW, Reichner J, Simms HH, et al.: Shock-induced neutrophil

- mediated priming for acute lung injury in mice: divergent effects of TLR-4 and TLR-4/FasL deficiency. *Am J Pathol* 161(6):2283–2294, 2002.
17. Maeshima K, Takahashi T, Uehara K, Shimizu H, Omori E, Yokoyama M, Tani T, Akagi R, Morita K: Prevention of hemorrhagic shock-induced lung injury by heme arginate treatment in rats. *Biochem Pharmacol* 69(11):1667–1680, 2005.
 18. Van Rhijn I, Rutten VP, Charleston B, Smits M, van Eden W, Koets AP: Massive, sustained gammadelta T cell migration from the bovine skin *in vivo*. *J Leukoc Biol* 81(4):968–973, 2007.
 19. Egan PJ, Kimpton W, Seow HF, Bowles VM, Brandon MR, Nash AD: Inflammation-induced changes in the phenotype and cytokine profile of cells migrating through skin and afferent lymph. *Immunology* 89(4):539–546, 1996.
 20. Li Z, Burns AR, Han L, Rumbaut RE, Smith CW: IL-17 and VEGF are necessary for efficient corneal nerve regeneration. *Am J Pathol* 178(3):1106–1116, 2011.
 21. Byeseda SE, Burns AR, Dieffenbaugher S, Rumbaut RE, Smith CW, Li Z: ICAM-1 is necessary for epithelial recruitment of gammadelta T cells and efficient corneal wound healing. *Am J Pathol* 175(2):571–579, 2009.
 22. Purcell EM, Dolan SM, Kriynovich S, Mannick JA, Lederer JA: Burn injury induces an early activation response by lymph node CD4⁺ T cells. *Shock* 25(2):135–140, 2006.
 23. Rani M, Zhang Q, Scherer MR, Cap AP, Schwacha MG: Activated skin $\gamma\delta$ T-cells regulate T-cell infiltration of the wound site after burn. *Innate Immun* 21(2):140–150, 2015.
 24. Shah D, Romero F, Stafstrom W, Duong M, Summer R: Extracellular ATP mediates the late phase of neutrophil recruitment to the lung in murine models of acute lung injury. *Am J Physiol Lung Cell Mol Physiol* 306(2): L152–L161, 2014.
 25. Makarenkova VP, Bansal V, Matta BM, Perez LA, Ochoa JB: CD11b⁺/Gr-1⁺ myeloid suppressor cells cause T cell dysfunction after traumatic stress. *J Immunol* 176(4):2085–2094, 2006.
 26. Zhang K, Bai X, Li R, Xiao Z, Chen J, Yang F, Li Z: Endogenous glucocorticoids promote the expansion of myeloid-derived suppressor cells in a murine model of trauma. *Int J Mol Med* 30(2):277–282, 2012.
 27. Rani M, Zhang Q, Schwacha MG: Gamma delta T cells regulate wound myeloid cell activity after burn. *Shock* 42(2):133–141, 2014.
 28. Mendoza AE, Neely CJ, Charles AG, Kartchner LB, Brickey WJ, Khoury AL, Sempowski GD, Ting JP, Cairns BA, Maile R: Radiation combined with thermal injury induces immature myeloid cells. *Shock* 38(5):532–542, 2012.
 29. Boismenu R, Feng L, Xia YY, Chang JC, Havran WL: Chemokine expression by intraepithelial gamma delta T cells. Implications for the recruitment of inflammatory cells to damaged epithelia. *J Immunol* 157(3):985–992, 1996.
 30. Jameson JM, Cauvi G, Sharp LL, Witherden DA, Havran WL: Gammadelta T cell-induced hyaluronan production by epithelial cells regulates inflammation. *J Exp Med* 201(8):1269–1279, 2005.

